Superconductive PT-symmetry phase transition in metasurfaces

Wang, Dongyang; Li, Chun; Zhang, Caihong; Kang, Ming; Zhang, Xueqian; Jin, Biaobing; Tian, Zhen; Li, Yanfeng; Zhang, Shuang; Han, Jiaguang; Zhang, Weili

DOI:
10.1063/1.4973769
10.1063/1.4973769

Superconductive PT-symmetry phase transition in metasurfaces

Dongyang Wang,[1,4] Chun Li,[2] Caihong Zhang,[2,a)] Ming Kang,[3] Xueqian Zhang,[1] Biaobing Jin,[2] Zhen Tian,[1] Yanfeng Li,[1] Shuang Zhang,[4] Jiaguang Han,[1,b)] and Weili Zhang[1,5, c)]

[1] *Center for Terahertz Waves and College of Precision Instrument and Optoelectronics Engineering, Tianjin University, Tianjin 300072, China*

[2] *Research Institute of Superconductor Electronics, Nanjing University, Nanjing 210093, China*

[3] *College of Physics and Materials Science, Tianjin Normal University, Tianjin 300387, China*

[4] *School of Physics and Astronomy, University of Birmingham, Birmingham, B15 2TT, UK*

[5] *School of Electrical and Computer Engineering, Oklahoma State University, Stillwater, Oklahoma 74078, USA*

We experimentally demonstrate a dynamic process of effective Parity-Time (PT)-symmetry breaking through eigen-polarization variation in a hybridized metasurface. The metasurface consists of two coupled resonators made from metal and type II superconductor niobium nitride, respectively. By varying the temperature from 2 to 13 K, the hybridized system is able to pass through the effective PT-symmetry phase transition point, providing a feasible way to investigate the dynamic PT-symmetry transition.

[a)] Electronic mail: chzhang@nju.edu.cn
[b)] Electronic mail: jiaghan@tju.edu.cn
[c)] Electronic mail: weili.zhang@okstate.edu

Parity-Time (PT)-symmetric Hamiltonians, first proposed by Bender in 1998,[1] describe a class of non-Hermitian quantum systems obeying parity-time requirements. Even being non-Hermitian systems, the PT-symmetric Hamiltonians can still possess a real and complete eigen-spectrum due to critical requirement of PT symmetry, and therefore satisfy the necessary physical constraints for measurable quantities. Since then, such Hamiltonians have attracted tremendous interest in the past two decades, and have led to many interesting developments in theoretical physics.[2] Due to difficulties in engineering complex PT-symmetric potentials, experimental observation of the PT-symmetric systems in quantum mechanics has been very scarce.[1,2] As electromagnetic and quantum waves obey similar mathematical forms of wave equations, the concept of PT symmetry has been introduced in optical systems with spatially balanced refractive index profiles.[3,4] Spontaneous PT-symmetry breaking separated by the transition point, i.e., exceptional point, has been experimentally demonstrated in various optical systems, in which a complex conjugate refractive index profile is usually employed to construct analog PT-symmetric quantum potentials. Many intriguing optical phenomena related to the PT symmetry have been observed, such as loss-induced transparency, asymmetric light propagation, one way invisibility, *etc*.[4-9] In most of the demonstrations, discrete optical elements such as waveguides and resonators with mutual coupling have been employed, and the system can be mathematically described by an effective Hamiltonian of matrix representation with off-diagonal elements representing the coupling coefficients.[4] A transition between PT symmetry and PT-symmetry breaking can be observed by carefully tuning the relative strength between the loss contrast and the coupling coefficient.

Instead of generating the complex refractive index profiles under the requirement of PT symmetry, metasurfaces consisting of coupled resonators with contrasting quality factors have been employed to generate effective Hamiltonians satisfying PT symmetry.[10, 11] In one case, the effective PT symmetry of the Hamiltonian was built by two coupled dipole antennas with the same resonance frequency and scattering loss rate, but different dissipation loss rates. The orthogonality between the two antennas not only ensures a real coupling constant between them, but also, under such a requirement, the eigen-polarization states in transmission can directly indicate the signature of transition at the exceptional point. The coupling strength between the two dipoles, which is determined by their separation, was usually selected as the tuning parameter. In order to reveal the process of the PT-symmetry phase transition, a series of samples with different separations between the two antennas need to be fabricated and measured. Due to the fixed structure, each sample thus has a fixed optical response without any dynamical modulation.

To be able to continuously control the transition through the exceptional point dynamically, here, we incorporate superconducting material into the PT-symmetry metasurface design. The unit cell of the hybridized metasurface also consists of two resonators, one made from Au, while the other from type II superconductor niobium nitride (NbN). Due to the presence of the type II superconductor, the dissipation loss of the NbN resonator can be actively controlled by tuning the temperature, the strength of the magnetic or electric field.[12-16] With the proper design of the metasurface, dynamic tuning of the dissipation loss of NbN can lead the system to continuously pass through the effective PT- symmetry phase transition point in the fabricated sample. By only changing the temperature from 2 to 13 K, we experimentally observed such a phase transition manifested in the measured eigen-polarization variation in transmission. A coupled mode analysis is used to explain the experimental results.

Similar to our previous work,[11] the metamaterial implementing PT-symmetry phase transition also contains two split-ring resonators (SRRs) acting as effective dipoles $\hat{p}_{x,y} = \tilde{p}_{x,y}(\omega)e^{i\omega t}$ with the same resonance frequency ω_0 and their gaps are orthogonal to each other, as shown in Fig. 1(a). Although the SRRs also support magnetic dipole moments in the vertical direction, they do not make the far-field contribution under normal incidence. These dipoles are excited by the incoming electric field $\hat{E}_0 = (\tilde{E}_x, \tilde{E}_y)e^{i\omega t}$, as given by the following equation [10,11]

$$\Omega\begin{pmatrix}\tilde{p}_x\\ \tilde{p}_y\end{pmatrix} = \begin{pmatrix}\delta + i\gamma_x & \kappa\\ \kappa & \delta + i\gamma_y\end{pmatrix}\begin{pmatrix}\tilde{p}_x\\ \tilde{p}_y\end{pmatrix} = \begin{pmatrix}\sqrt{\gamma_x^s} & 0\\ 0 & \sqrt{\gamma_y^s}\end{pmatrix}\begin{pmatrix}\tilde{E}_x^i\\ E_y^i\end{pmatrix}, \tag{1}$$

where $\gamma_{x,y} = \gamma_{x,y}^s + \gamma_{x,y}^d$ is the total decay rate for each dipole, $\gamma_{x,y}^s$ is the scattering loss rate considered to be approximately the same for the two SRRs here, and $\gamma_{x,y}^d$ is the dissipation loss, which is different in the two SRRs due to their different geometries and constituent materials. The frequency deviation δ satisfies the requirement of $\delta = \omega - \omega_0 \ll \omega_0$, and κ denotes the coupling between the resonators and should be real since the coupling between the two dipoles only interact via quasi static electric field. These dipoles reradiate the EM wave to the far-field as:

$$\sqrt{\gamma_s}\begin{pmatrix}\tilde{p}_x\\ \tilde{p}_y\end{pmatrix} + \begin{pmatrix}1 & 0\\ 0 & 1\end{pmatrix}\begin{pmatrix}\tilde{E}_x^i\\ \tilde{E}_y^i\end{pmatrix} = \begin{pmatrix}\tilde{E}_x^t\\ \tilde{E}_y^t\end{pmatrix}. \tag{2}$$

Thus, the transmitted and incident fields can be related by the transmission matrix, **T**:

$$T = \sqrt{\gamma^{s}} \begin{pmatrix} \delta + i\gamma_s & \kappa \\ \kappa & \delta + i\gamma_y \end{pmatrix}^{-1} \sqrt{\gamma_s} \; . \tag{3}$$

Under the requirement of the same scattering loss rate and the same resonance frequency, the eigenvalue problem of the transmission matrix **T** of the metasurface is equivalent to that of the response matrix **Ω**. Since that, instead of investigating the eigenvalues of the response matrix, we can directly investigate the eigenvalue problem of the matrix **T** by spectral measurement to reveal the PT-symmetry breaking process. Solving the eigenvalues of **T** reveals the constraint of phase transition, which depends on the value of $\Delta = \sqrt{4\kappa^2 - \left(\gamma_x^d - \gamma_y^d\right)^2}$. Hence by carefully tuning the dissipation loss rate of the type II superconductor NbN, γ_x^d, while keeping the other parameters constant, the effective PT- symmetry breaking point $\Delta = 0$ can be reached. Ideally, above the transition point, $\Delta > 0$, the eigen-polarizations of the transmission matrix **T** are two ellipses with major axes oriented along ±45° in the form of $x \pm e^{\pm i\theta} y$, where $\theta = \sin^{-1}\left[\left(\gamma_x^d - \gamma_y^d\right)/2\kappa\right]$. When $\Delta = 0$, i.e., at the exceptional point, the eigen-polarizations are collapsed to a single circularly polarized state, either left-handed or right-handed circular polarization, which is determined by microscopic parameters. When Δ is purely imaginary, the eigen-polarizations are two ellipses with major axes oriented along 0° and 90° with the form of $x \mp ie^{\theta} y$, where $\theta = \cosh^{-1}\left[\left(\gamma_x^d - \gamma_y^d\right)/2\kappa\right]$. These eigen-polarization states originated from the effective PT-symmetry transition can be adjusted by directly tuning γ_x^d, and reveal the phase transition at the same time.

To experimentally verify such an effective PT phase transition, we fabricate the metasurface with carefully designed parameters by photolithography. We first etch the 50 nm NbN film grown on 1 mm MgO substrate into an array of SRRs, and then the other metal dipole is steamed with Au to 200 nm. The unit cell has a period of 120 μm in both directions, and the overall sample area is 10 mm by 10 mm. The detailed geometry of the resonators is shown in Fig. 1. A series of samples with slightly different geometric parameters are fabricated to identify the best candidate. In order to obtain both the amplitude and phase information of the metamaterial response, we measure the transmission spectrum of our samples with terahertz time-domain spectroscopy coupled with a He-bath cryostat (Oxford Instruments Spectromag). The liquid helium circulation in the cryostat provides adjustable temperature from 1.5 to 250 K and ensures an accuracy of 0.01 K during the measurement. As shown in Fig. 2, the two terahertz antennas are oriented to measure the horizontally polarized terahertz wave in our experiment setup, and the samples are placed 45° relative to the horizontal direction. Four polarization plates are used in the experiment to measure each element of the transmission matrix **T**. The transmission coefficients are normalized by the transmissions of the MgO substrate. By carefully tuning the temperature, the transmission of the sample at different temperatures can be measured, and the transmission coefficients can be theoretically fitted according to Eq. 3. Figure 3 shows the experimental and fitted transmission matrix elements at 7 K. The near-field coupling between these SRRs generally leads to polarization state change through the sample due to the non-zero crossed linear polarization components. Since the geometry of the dipoles and the distance between them do not change with temperature, the fitted scattering loss rate and the coupling strength are assumed to be constant. Furthermore, the dissipation loss of Au is not sensitive to temperature and can also be assumed to be constant. To ensure a sharp change in dissipation of NbN, the investigated temperature here is chosen to be around 10 K, which lies in the temperature-sensitive region of NbN. The parameters can be obtained by numerically fitting the measured transmission spectra at each temperature based on Eq. 3. According to the transmissions at different temperatures, the dependence of the fitted dissipation loss rate of the NbN resonator on temperature is plotted in Fig. 4(a), where a sharp change occurs around 10 K. We find that the resonance frequency of the NbN resonator is also slightly changed in the temperature-sensitive region, as shown in Fig. 4(b). The slightly changed resonance frequency leads to deviation from the PT symmetry requirement above 9 K. In the temperature-sensitive region of the NbN resonator, the microscopic parameter, namely, the dissipation loss rate, shows an obvious change.

Based on the measured elements of the transmission matrix **T** (including amplitude and phase), we can directly obtain its eigen-polarization states at each temperature. As shown in Fig. 5, we plot the fitted and measured eigen-polarization states of the transmission matrix **T** from 7 to 12 K. Below 9 K, the major axes of the eigen-polarization states are close to ± 45° directions, which reveal that the hybridized system falls into the PT-symmetry phase region. However, the major axes of the eigen-polarization states are rotated and close to 0° and 90° directions when the temperature is above 9 K, which directly indicates the breaking of the PT symmetry. Around

9 K, the eigen-polarization states are approximately going to collapse to circular polarization, indicating proximity to the exceptional point. Due to the resonant frequency deviation of the NbN resonator above 9 K, the major axes of the eigen-polarization states show slight deviation from 0° and 90° directions. Further, in Fig. 5(k) we plot the experimentally measured eigen-polarization states on the Poincare sphere, where the process of transition can be represented by the approaching and leaving the EP point located at the north pole of the Poincare sphere. The two coloured longitudes represent the coordinate with a bit of shift for legibility which corresponds to a rotation of transmission matrix **T**. It must be noted that the eigen-polarization states of the transmission matrix are elliptically-polarized states with the same chirality due to the critical requirement of mirror symmetry along the propagation direction for the response matrix.[17, 18]

In conclusion, we have designed and experimentally fabricated a hybridized metasurface exploring effective PT-symmetry phase transition. To avoid the requirement of a series of samples, the dissipation loss rate of one dipole is selected as the tuning parameter, and can be continuously tuned by changing the environmental temperature. To realize the tuning process in concrete metamaterial design, a temperature-sensitive type II superconductor resonator is implemented. By changing the environmental temperature from 7 to 12 K, phase transition in the polarization space is experimentally observed. The proposed structure may be used in the low-noise terahertz receiver system, such as the NbN hot electron bolometer (HEB), and the thermal-control strategy also could be extended to other thermo-responsive materials.

Acknowledgements

This work was supported by the National Key Basic Research Program of China (Grant No. 2014CB339800), the National Science Foundation of China (61307125, 61427814, 61422509, 61420106006, 61328503, 61205098); Program for Changjiang Scholars and Innovative Research Team in University, "PCSIRT"(IRT13033); the U.S. National Science Foundation (Grand No. ECCS-1232081), the Major National Development Project of Scientific Instruments and Equipment (Grant No. 2011YQ150021).

References:

[1] C. M Bender and S. Boettcher, Phys. Rev. Lett. **80**, 5243 (1998).

[2] C. M. Bender, D.C. Brody, and H. F. Jones, Am. J. Phys. **71**, 1095 (2003).

[3] R. El-Ganainy, K. G. Makris, D. N. Christodoulides, and Ziad H. Musslimani, Opt.Lett. **32**, 2632 (2007).

[4] A Guo, G J Salamo, D Duchesne, R Morandotti, M Volatier-Ravat, V Aimez, G A Siviloglou, and D N Christodoulides, Phys. Rev. Lett. **103**, 093902 (2009).

[5] K GMakris, R El-Ganainy, D NChristodoulides, and Z H Musslimani, Phys. Rev. Lett. **100**, 103904 (2008).

[6] C. E Rüter, K. G Makris, R. El-Ganainy, D. N Christodoulides, M. Segev, and D. Kip, Nat. Phys. **6**, 192 (2010).

[7] B. Peng, S. K.Özdemir, F. Lei, F. Monifi, M. Gianfreda, G. L. Long, S. Fan, F.Nori, C. M. Bender, and L. Yang, Nat. Phys. **10**, 394 (2014).

[8] Z. Lin, H. Ramezani, T. Eichelkraut, T. Kottos, H. Cao, and D. N. Christodoulides, Phys. Rev. Lett. **106**, 213901 (2011).

[9] X. Zhu, L. Feng, P. Zhang, X. Yin, and X. Zhang, Opt.Lett. **38**, 2821 (2013).

[10] M. Kang, F. Liu, and J. Li, Phys. Rev. A. **87**, 053824 (2013).

[11] M. Lawrence, N. Xu, X. Zhang, L. Cong, J. Han, W. Zhang, and S. Zhang, Phys. Rev. Lett. **113**, 093901 (2014).

[12] C. Zhang, B. Jin, J. Han, I. Kawayama, H. Murakami, J. Wu, L. Kang, J. Chen, P. Wu, and M.

Tonouchi, Appl. Phys. Lett. **102**, 081121 (2013).

[13] J. Gu, R. Singh, Z. Tian, W. Cao, Q. Xing, M. He, J. W. Zhang, J. Han, H-T. Chen, and W. Zhang, Appl. Phys. Lett. **97**, 071102 (2010).

[14] L. P. Hari, J. Rubinstein, and P. Sternberg, Physica D: Nonlinear Phenomena **261**, 31 (2013).

[15] M. C. Ricci, H. Xu, R. Prozorov, A. P. Zhuravel, A. V. Ustinov, and S. M. Anlage, IEEE Trans. Appl. Superconductivity **17**, 918 (2007).

[16] D. Wang, Z. Tian, C. Zhang, X. Jia, B. Jin, J. Gu, J. Han, and W. Zhang, J. Opt. **16**, 094013 (2014).

[17] H. Cao and J Wiersig, Rev. Mod. Phys. **87**, 61 (2015).

[18] M. Kang, J. Chen, and Y. D. Chong, Phys. Rev. A **94**, 033834 (2016).

Figures

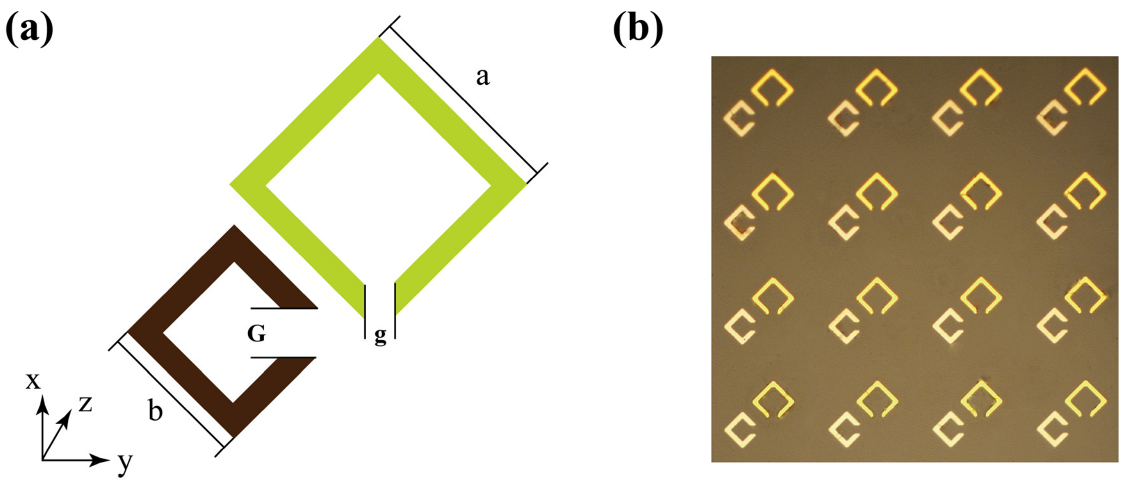

FIG. 1. (a) Schematic of a unit cell of the proposed metasurface. The parameters used in simulation are a = 42 μm, b = 30 μm, g = 6 μm, G = 10 μm. (b) Microscopy image of the sample measured in experiments.

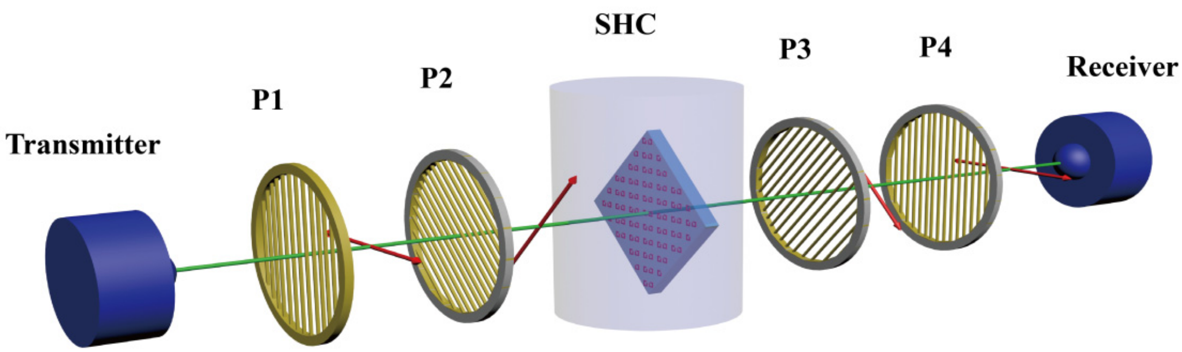

FIG. 2. Experimental diagram for the terahertz transmission matrix measurements.

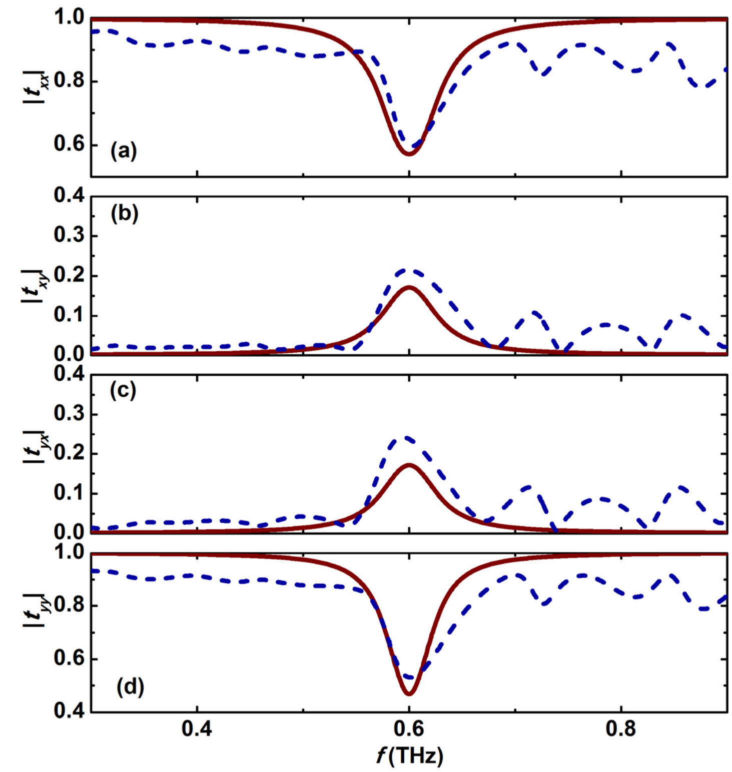

FIG. 3. Experimental (dash lines) and fitted (solid lines) transmission spectra at 7 K. The fitted microscopic parameters are $f_x = f_y = 0.6$ THz, $\gamma^s = 0.015$ THz, $\gamma_x^d = 0.016$ THz, $\gamma_y^d = 0.01$ THz, and $\kappa = 0.01$ THz.

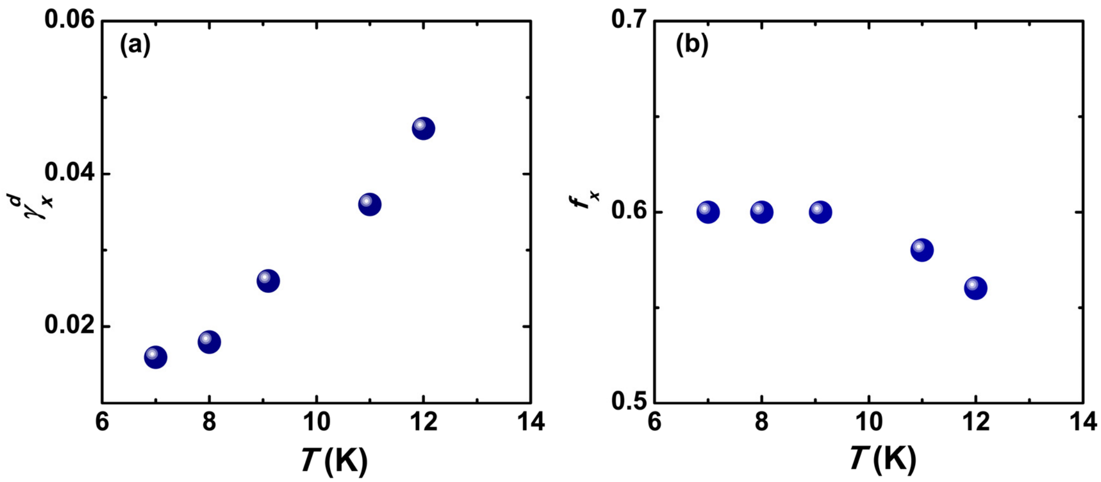

FIG. 4. Fitted (a) dissipation loss rate γ_x^d and (b) resonance frequency f_x of the NbN resonator from 7 to 12 K.

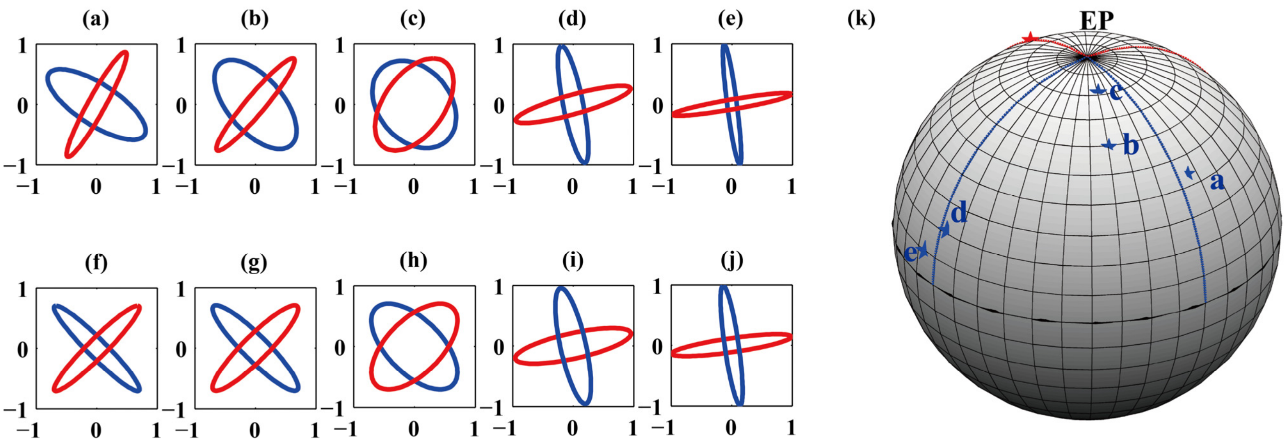

FIG. 5. Eigen-polarization states of the transmission matrix in polarization space. The eigen-polarization states in the first row are the experimental results, and those in the second row are the corresponding fitted results: (a) and (f) T = 7 K, (b) and (g) T = 8 K, (c) and (h) T = 9.1 K, (d) and (i) T = 11 K, and (e) and (j) T = 12 K. And (k) is the Poincare sphere presentation of transition from (a) to (e).